

Geochemical characteristics of mafic and ultramafic rocks from the Naujat anorthosite complex, southern West Greenland

Mineral resource assessment of the
Archaean Craton (66° to 63°30'N)
SW Greenland Contribution no. 7

Henrik Solgevik, J. Ellis Hoffmann
& Anders Scherstén



GEOLOGICAL SURVEY OF DENMARK AND GREENLAND
MINISTRY OF CLIMATE AND ENERGY



G E U S

Geochemical characteristics of mafic and ultramafic rocks from the Naujat anorthosite complex, southern West Greenland

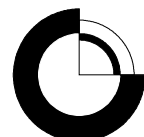
Mineral resource assessment of the
Archaean Craton (66° to 63°30'N)
SW Greenland Contribution no. 7

Henrik Solgevik¹, J. Ellis Hoffmann²
& Anders Scherstén³

¹Stockholm University, Sweden

²Universität Bonn, Germany

³Geological Survey of Denmark and Greenland (GEUS)



Contents

Abstract	3
Introduction	4
Background.....	4
Regional geology	5
Lithologies and samples.....	7
Amphibolites.....	7
Ultramafics	7
Anorthosites	7
Geochemistry	9
Analytical methods	9
Results - Geochemical characterization	13
Amphibolites.....	13
Ultramafic rocks.....	18
Anorthosites	20
Discussion	21
Alteration.....	21
Major, trace and rare earth elements	22
Summary	24
Acknowledgements	25
References	26

Abstract

The Naujat anorthosite complex, SW Greenland consists of a large body of gabbro-leucogabbro-anorthosite, amphibolites arranged in up to 200 meter wide and kilometres long layers and a variety of ultramafic rocks intimately associated with the amphibolites. They have all been intruded by Tonalite-trondhjemite-granodiorite (TTG) associations and are folded on a large scale. Thirty-four samples from all three melanocratic-ultramafic rock types have been analysed for major and trace element concentrations.

The amphibolites correspond to tholeiitic basalts with 5.2-9.7 wt.% MgO, Mg# 44-61 and 46–50 wt.% SiO₂ and relatively flat chondrite normalised rare-earth-element (REE) patterns. Negative Th anomalies and weak negative Zr and Ti anomalies in a primitive mantle-normalised trace element diagram are interpreted to show a subduction imprint in terms of a subduction related origin of these rocks. The ultramafic rocks have 23-48 wt.% MgO, Mg# 77-91 and 40-49 wt.% SiO₂ and are modally classified as dunites, hartzburgites, lherzolites and olivine-websterites. They also have relatively flat REE patterns, but with slightly enriched heavy-rare-earth-elements (HREE) over LREE. The REE and spider diagrams reflect olivine crystal fractionation from depleted dunites to slightly enriched lherzolites (compared to the dunites) and variable positive and negative anomalies for Nb, Sr, Eu and Ti. Anorthosites are characterized by 48-52 wt.% SiO₂, 13.5-15.5 wt.% CaO, 2-5 wt.% Na₂O and REE and spider diagrams showing enriched LREE and relatively flat to depleted HREE with negative Nb, Zr and Ti and positive Sr and Eu. MgO variation diagrams for all three lithological units are consistent with plagioclase and olivine fractionation.

Our present interpretation is that the amphibolites represent former oceanic crust (N-MORB) intruded by the gabbro-anorthosite complex which fractionated into cumulates, gabbros, leucogabbros and anorthosites followed by subduction or melting of a thickened oceanic crust.

Introduction

This report is a geochemical complement to the GEUS report “Magmatic environment: The Naujat gabbro-anorthosite complex and country rocks – Field report 2006” by Frei & Konnerup-Madsen (2007). The aim of the report from Frei and Konnerup-Madsen was to map and describe the lithological relationships in a specific magmatic environment in the geological map-sheet Kapisillit 64 V2 Syd (in preparation) and to assess its possible economic mineral potential.

The Naujat area consists dominantly of a layered mafic and ultramafic complex with a kilometre-scale gabbro-anorthosite body and closely related amphibolites and ultramafic rocks. The mafic rocks range from leucocratic amphibolite and homogeneous amphibolite to heterogeneous amphibolite and occur as up to 200 m thick layers that are traceable for kilometres along strike of foliation (Frei & Konnerup-Madsen, 2007). A large variety of ultramafic rocks are found that are associated with the amphibolites and possibly with the anorthosite suite. The amphibolitic and ultramafic layers and pods show a variable degree of strain and alteration, from nearly undeformed and unaltered to highly strained and metasomatised layers. The area has been large-scale folded and partly broken up by intrusive sheets of tonalites, granodiorites and minor granites.

We have performed whole-rock analyses on mafic and ultramafic rocks collected by Frei and Konnerup-Madsen in 2006 and Solgevik and Piazolo, 2005. This report aims to describe the geochemical characteristics of the mafic and ultramafic rocks and to infer their likely origin and geological environment in which they were formed.

Background

From 2004 to 2007 GEUS has investigated various aspects of the geology of supracrustal belts in the Nuuk region, in particular focussing on understanding aspects of the primary geological environments and their mineral occurrences, geological setting, and alteration patterns. Detailed mapping of key areas in 2004, 2005, 2006 and 2007 and targeted geochemistry and geochronology has identified Mesoarchaean greenstone belts. Understanding the primary greenstone-granite environment of these supracrustal rocks and the alteration patterns is important in relation to understand the formation of mineral occurrences (Stendal 2007). However, it is complicated by 1) the rarity of preserved primary structures due to hydrothermal alteration, metamorphism, and multiple deformation events; and 2) the recognition of tectonic imbrications probably of rocks of widely different ages, and which might be formed in different geological environments. To solve some of these difficulties, field work was carried out in different key areas and this study presents the geochemical interpretation of an anorthosite complex at Naujat. This project is co-financed between Bureau of Mines and Petroleum (BMP), Government of Greenland and GEUS.

Regional geology

The Naujat anorthosite complex is located at the tip of the Ameralik fjord south of Nuuk, SW Greenland (Fig. 1) and occurs within the Archaean craton. The regional geology consists, according to several authors (e.g Friend and Nutman, 2005), of different terranes with separated ages and tectonothermal histories. The area in which the Naujat anorthosite complex is located has so far been outside the terrane model based on field evidence, but is inferred to belong to the Tre Brødre terrane (Friend and Nutman, 2005). The regional geology concerning the Kapsillit map-sheet in the area have been mapped during field seasons 2005-2007 by GEUS and is currently being compiled and interpreted. From the regional map of Escher and Pulvertaft (1995) there is an inferred terrane boundary to the south of the Naujat anorthosite complex under the glacier tongue separating the Tasiussarsuaq terrane in the south from the Tre Brødre terrane in the north (Fig. 1).

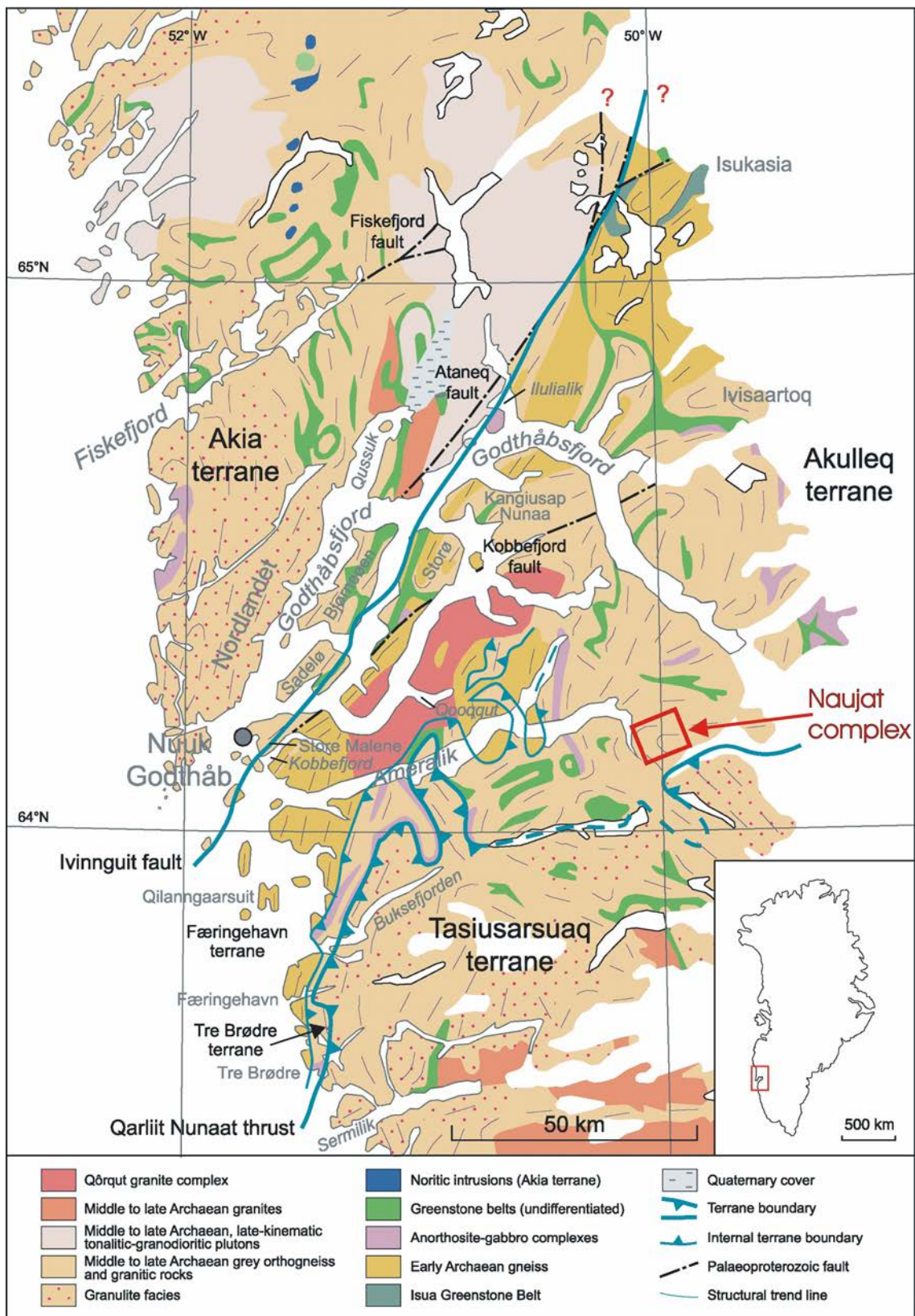


Figure 1. Geological map of the Nuuk region, SW Greenland, with location (red box) of the Naujat anorthosite complex. Modified from Garde (2003) after Escher and Pulvertaft (1995).

Lithologies and samples

Amphibolites

The amphibolites consist of amphibole + plagioclase +/- pyroxene +/- garnet +/- biotite +/- olivine. The amount of modal plagioclase varies and one sample (df 496605) is classified (in the field) as leucocratic amphibolite (Table 1 in Frei and Konnerup-Madsen, 2007). Some outcrops with coarse grained homogeneous amphibolite display a magmatic gabbroic texture (Fig. 2a) while some outcrops consists of a more heterogeneous amphibolite (Fig. 2b) with cm-dm scale compositional variations. Thus, some of the amphibolites are interpreted to be mafic volcanics. Several samples are garnet-bearing and will be further analysed for PT estimates. Amphibolites in the central and eastern part of the area have partial melt-pockets with garnets and greenish clinopyroxenes in contrast to the most western parts which also have partial melts with brownish orthopyroxenes.

Ultramafics

The ultramafic units occur with a large compositional variety (Frei & Konnerup-Madsen, 2007) from massive dunitic pods with a yellow-brownish weathering crust (Fig. 2c) to darker, layered outcrops (Fig. 2d). Several of the ultramafic outcrops display cumulate textures (Fig. 2e) and the alteration and strain is very varied throughout the mapped area.

According to the classification scheme of LeMaitre (1989), the ultramafic samples are modally classified as dunites, hartzburgites, spinel-Iherzolites, garnet-Iherzolite and olivine-websterite. Four samples are too altered in thin section to be classified (Table 1). Dark green spinel is abundant in several samples classified as spinel-Iherzolites (Table 1) where one Iherzolite (df496617; Table 1) possibly has garnet growing on the expense of orthopyroxene. Plagioclase is rare and some of the samples do not contain any plagioclase. Accessory minerals are commonly magnetite, chromite and in some cases ilmenite. Calcite is found in one of the more altered samples. Serpentisation is rare among the least altered samples and occurs only in small scale alteration along a few grain boundaries.

Anorthosites

The kilometer-scale leucogabbro-anorthosite body dominantly consists of coarse grained plagioclase + amphibole +/- pyroxene +/- biotite +/- quartz +/- garnet. The modal amount of mafic minerals varies on outcrop scale and the classification range from dominantly leucogabbro – anorthosite (Fig. 2f) to rare gabbro. The amount of quartz may occasionally be significantly high (> 5 %) close to and inside high strained parts of the anorthosite-leucogabbro-gabbro suite and suggests movements of silica-rich fluids during deformation and metamorphic events and possibly the breakdown of orthopyroxene. Sample df496647 is, compared to other associated samples from the same suite, enriched in quartz.

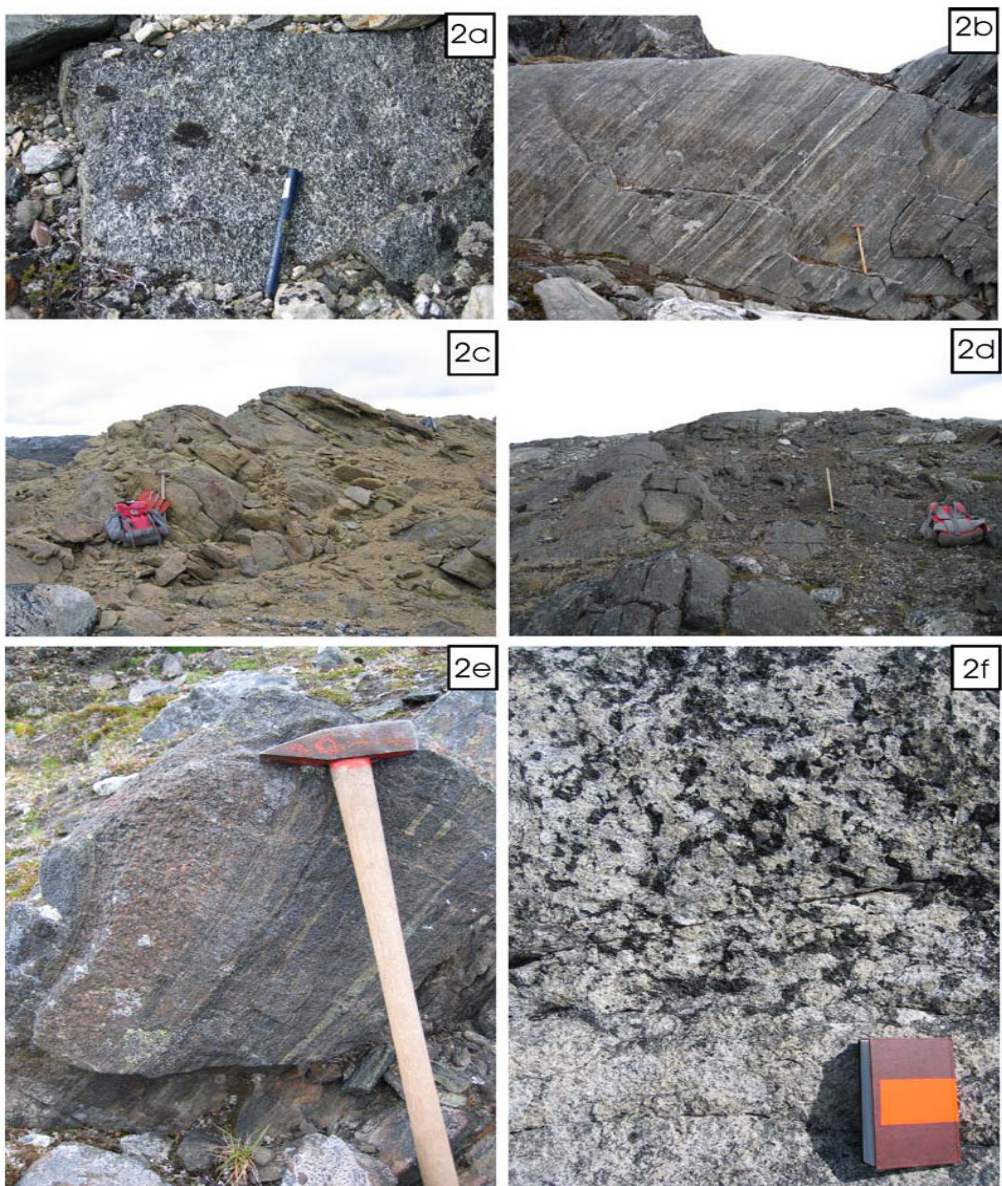


Figure 2. Representative photos of mafic-ultramafic lithologies. **a)** coarse grained homogeneous amphibolite. **b)** heterogeneous amphibolite. **c)** massive dunitic pods. **d)** dark layered ultramafic outcrops of spinel-lherzolite. **e)** strained ultramafic outcrop with cumulate textures. **f)** leucogabbro grading into anorthosite composition.

Geochemistry

Analytical methods

Whole-rock geochemical analyses for major and trace elements were performed on seventeen ultramafic rocks, three anorthosites and fourteen amphibolites. The results are shown in Table 1. All samples were grounded using tungsten carbide mills at either GEUS (Geological Survey of Denmark and Greenland) in Copenhagen or at Stockholm University, Sweden. Major elements were determined on fused glass discs (sample powder fluxed with sodium tetraborate, ratio 1:7) using a Philips PW1606 multichannel X-ray fluorescence (XRF) at GEUS. Na₂O and Cu were determined by atomic absorption spectrometry (AAS). A complete description of the XRF analytical procedure is described by Kystol and Melchior Larsen (1999). Trace elements were analysed at GEUS using a PerkinElmer Elan 6100DRC ICP-MS instrument. Analyses were made on dissolved pieces of the borate glass discs from each sample used for major element XRF analysis. International standards BHVO-2 and GH were used as reference materials, along with the in-house standard Disko-1, to estimate precision and accuracy during the ICP-MS procedure.

Table 1.

Major (wt%) and trace (ppm) element concentrations of mafic and ultramafic rocks from the Naujat Anorthosite complex.

Sample	Ultramafic											
	df496604	df496617	df496619	df496621	df496628	df496632	df496633	df496638	df496639	df496640	df496641	df496648
	Alt	Gt-Iher	OI-web	Lher	Alt	dun	Hartz	Sp-Iher	Hartz	Sp-Iher	Sp-Iher	Sp-Iher
SiO ₂	44.82	47.33	45.16	42.26	49.71	44.02	46.33	47.32	45.92	48.77	46.42	46.84
TiO ₂	1.87	0.17	0.36	0.18	0.91	0.14	0.19	0.34	0.16	0.17	0.32	0.34
Al ₂ O ₃	11.66	3.83	9.39	3.70	10.25	2.64	3.80	8.33	3.55	5.02	6.85	7.53
FeO	5.33	2.07	3.99	1.69	5.06	2.93	1.66	4.50	3.40	3.25	4.00	3.66
FeOt	11.84	4.89	8.47	7.58	6.06	7.56	8.14	6.32	6.00	5.33	5.58	7.27
MnO	0.22	0.12	0.20	0.13	0.16	0.19	0.22	0.18	0.14	0.15	0.16	0.19
MgO	9.34	36.07	22.79	36.92	11.52	37.69	30.20	23.47	36.69	30.26	28.24	24.91
CaO	9.43	0.91	6.26	2.94	11.79	1.14	6.04	6.71	0.68	4.77	5.56	6.34
Na ₂ O	1.69	0.10	0.76	0.34	0.06	0.15	0.25	0.42	0.07	0.22	0.50	0.36
K ₂ O	0.67	0.02	0.12	0.40	0.02	0.41	0.05	0.05	0.01	0.03	0.07	0.07
P ₂ O ₅	0.26	0.01	0.02	0.01	0.07	0.01	0.01	0.03	0.00	0.02	0.02	0.02
LOI	2.18	3.51	1.06	2.37	3.67	1.59	1.51	0.89	2.54	0.84	0.89	1.17
Sum	99.30	99.03	98.58	98.52	99.28	98.46	98.40	98.56	99.15	98.83	98.62	98.70
Mg#	50.00	90.50	77.10	87.90	65.90	86.80	84.80	80.10	87.80	86.70	84.60	80.80
Sc	38	14	30	13	68	13	16	31	13	16	19	26
Ti	11,783	803	1,972	888	5,271	595	735	1,715	776	742	1,459	1,870
V	285	65	164	70	148	61	84	143	67	102	122	131
Cr	80	2,099	3,019	2,772	209	3,609	3,096	3,304	2,469	2,282	2,536	2,709
Mn	1,820	1,033	1,646	1,124	1,240	1,485	1,737	1,429	1,131	1,198	1,294	1,525
Co	83	87	101	114	47	108	112	98	105	89	94	102
Ni	210	2,234	887	1,924	112	2,161	2,282	1,205	2,236	1,638	1,442	1,093
Cu	122	44	50	66	67	100	54	93	56	63	72	90
Zn	249	39	70	58	91	112	152	78	73	36	53	60
Ga	18.61	3.46	8.16	3.28	9.69	3.10	4.19	7.32	3.59	4.30	6.45	7.38
Rb	4.60	0.74	1.49	18.03	0.97	22.76	0.74	0.83	0.31	0.46	0.67	0.97
Sr	26.0	3.8	20.8	8.7	431.0	6.8	58.0	3.4	2.9	26.2	23.3	11.5
Y	33.93	3.70	8.77	3.86	21.40	2.69	4.54	8.40	2.26	4.78	8.73	8.34
Zr	133.31	8.68	16.82	8.41	53.08	5.66	11.24	16.22	6.38	9.03	20.51	21.04
Nb	6.15	0.39	0.79	0.56	3.03	0.38	0.53	0.69	0.32	0.45	0.87	0.81
Cs	0.37	0.11	0.07	1.81	0.03	2.18	0.04	0.02	0.02	0.02	0.02	0.05
Ba	71.05	0.11	9.80	4.64	13.63	7.77	37.88	1.18	1.37	4.77	5.40	0.87
Hf	3.29	0.26	0.49	0.22	1.58	0.19	0.31	0.47	0.20	0.28	0.57	0.64
Ta	0.91	0.13	0.51	0.22	0.57	0.32	0.38	0.49	0.26	0.56	0.26	0.23
Pb	2.14	0.54	1.33	1.04	1.53	1.37	6.26	0.63	0.25	0.68	0.62	0.86
Th	0.43	0.06	0.06	0.05	0.68	0.04	0.09	0.05	0.02	0.04	0.16	0.20
U	0.22	0.03	0.03	0.10	0.24	0.04	0.04	0.02	0.02	0.01	0.05	0.06
La	8.68	0.41	0.75	0.67	5.18	0.26	0.89	0.85	0.17	0.54	1.49	1.70
Ce	22.47	1.09	2.14	1.55	11.93	0.73	2.13	2.40	0.47	1.31	3.71	3.67
Pr	3.63	0.18	0.40	0.24	1.80	0.13	0.34	0.41	0.09	0.21	0.58	0.56
Nd	15.91	0.87	2.03	1.09	8.07	0.70	1.57	2.03	0.48	1.07	2.65	2.53
Sm	4.52	0.27	0.75	0.33	2.50	0.24	0.49	0.67	0.17	0.37	0.82	0.76
Eu	1.80	0.08	0.23	0.19	0.62	0.06	0.20	0.25	0.03	0.22	0.22	0.24
Gd	5.40	0.40	1.04	0.46	3.06	0.30	0.66	0.94	0.23	0.51	1.03	1.05
Tb	0.90	0.07	0.20	0.09	0.55	0.06	0.11	0.19	0.05	0.10	0.19	0.18
Dy	5.54	0.52	1.26	0.55	3.48	0.40	0.68	1.29	0.31	0.68	1.25	1.28
Ho	1.26	0.12	0.32	0.13	0.81	0.10	0.16	0.30	0.08	0.16	0.31	0.32
Er	3.39	0.35	0.85	0.34	2.22	0.28	0.44	0.82	0.24	0.46	0.83	0.87
Tm	0.53	0.06	0.13	0.06	0.35	0.05	0.07	0.14	0.04	0.08	0.14	0.14
Yb	3.34	0.38	0.90	0.39	2.28	0.28	0.43	0.90	0.26	0.51	0.88	0.91
Lu	0.52	0.06	0.14	0.06	0.34	0.04	0.07	0.14	0.04	0.08	0.14	0.14
(La/Yb)N	1.75	0.72	0.56	1.17	1.53	0.61	1.38	0.64	0.44	0.71	1.14	1.26
(La/Sm)N	1.21	0.94	0.63	1.26	1.30	0.67	1.15	0.80	0.63	0.90	1.15	1.41
(Gd/Yb)N	1.30	0.84	0.93	0.97	1.08	0.85	1.24	0.84	0.70	0.81	0.95	0.93
Ti/Ti*	0.95	0.93	0.85	0.87	0.75	0.87	0.50	0.83	1.54	0.65	0.62	0.81
Eu/Eu*	1.11	0.71	0.79	1.47	0.69	0.71	1.08	0.94	0.50	1.52	0.74	0.82
Nb/Nb*	1.30	1.05	1.51	1.20	0.66	1.65	0.79	1.33	2.25	1.27	0.72	0.57
Ti/Zr	88	92	117	106	99	105	65	106	122	82	71	89
Zr/Y	3.93	2.35	1.92	2.18	2.48	2.10	2.48	1.93	2.82	1.89	2.35	2.52
Al ₂ O ₃ /TiO ₂	6	22	26	21	11	20	20	25	22	29	21	22

Sample numbers are from GEUS database: df - Dirk Frei, hso - Henrik Solgevik, spi - Sandra Piazolo. Abbreviations: Alt - altered, Dun - dunite, Harz - hartzburgite, Lher - lherzolite, Sp-Iher - spinel-lherzolite, Gt-Iher - garnet-lherzolite, OI-web - olivine-websterite. Selected elements are chondrite normalized (N) using values of Boynton et al 1984. Mg# is 100*MgO/(MgO+FeO+Fetot) molecular ratio.

Table 1 continued.

Sample	Ultramafic				Anorthosite				Amphibolite			
	df496657	df496658	hs0485215	hs0485221	hs0485222	df496647	spi477950	spi477951	df496603	df496605	df496629	df496630
	Alt	Alt	Dun	Sp-her	Dun				Alt	prob alt	prob alt	
SiO ₂	52.25	40.59	40.70	46.45	40.41	51.85	48.90	47.82	36.37	46.63	47.44	48.16
TiO ₂	0.83	0.14	0.04	0.34	0.05	0.05	0.08	0.09	2.11	0.88	0.98	1.00
Al ₂ O ₃	18.81	2.51	0.58	8.55	0.75	29.72	31.87	31.37	9.19	23.54	15.44	17.46
Fe ₂ O ₃	6.53	2.67	1.14	3.60	1.39	0.79	0.53	0.29	12.08	2.03	3.37	2.17
FeO	0.00	5.70	7.39	7.47	6.61	0.00	0.59	1.20	9.82	5.30	8.53	9.68
FeOt	5.88	8.10	8.41	10.71	7.86	0.71	1.07	1.46	20.69	7.13	11.56	11.64
MnO	0.06	0.12	0.13	0.18	0.14	0.01	0.02	0.03	0.24	0.12	0.17	0.18
MgO	2.28	39.47	46.54	24.68	47.77	0.34	0.33	0.90	20.84	5.30	7.75	5.17
CaO	15.65	0.27	0.44	5.66	0.05	13.47	15.34	15.25	5.92	11.80	11.63	11.32
Na ₂ O	0.13	0.04	0.06	0.73	0.01	3.08	2.27	2.15	0.26	2.73	2.26	2.54
K ₂ O	0.19	0.17	0.01	0.11	0.01	0.21	0.19	0.32	0.07	0.23	0.23	0.37
P ₂ O ₅	0.18	0.01	0.01	0.04	0.01	0.01	0.01	0.01	0.98	0.01	0.07	0.08
LOI	3.15	7.12	2.11	1.16	1.68	0.73	0.45	0.63	1.49	1.30	1.56	1.27
Sum	100.05	98.82	99.15	98.96	98.86	100.27	100.58	100.07	99.37	99.87	99.41	99.40
Mg#	40.90	89.70	90.80	80.40	91.60	46.40	35.50	52.20	64.20	57.00	54.40	44.20
Sc	46	16	8	30	13	2	6	6	38	25	46	43
Ti	4,596	432	86	1,814	101	198	370	329	12,846	5,611	5,646	6,075
V	109	56	14	151	15	7	13	15	70	192	238	272
Cr	163	1,924	1,534	2,495	2,705	n.d.	8	3	11	108	294	184
Mn	494	1,122	1,031	1,475	1,125	88	147	244	1,989	1,053	1,315	1,365
Co	55	115	145	94	129	26	45	43	100	44	65	84
Ni	161	2,434	3,279	909	3,202	2	27	33	249	76	196	242
Cu	62	76	56	110	48	4	10	9	73	52	113	89
Zn	22	64	43	60	47	8	10	17	129	61	100	89
Ga	42.81	2.59	0.76	7.72	0.68	24.01	19.40	19.79	10.79	21.28	18.20	18.41
Rb	8.98	13.87	0.69	1.07	0.54	6.43	2.80	6.27	0.69	2.78	3.57	1.97
Sr	1,093.9	0.8	1.3	16.2	0.3	278.7	133.2	142.8	10.4	136.4	124.1	114.8
Y	27.04	2.46	0.87	8.72	0.41	0.78	2.85	1.47	35.06	10.87	20.73	20.99
Zr	537.44	6.00	1.29	21.48	0.83	6.12	7.31	2.98	132.98	25.81	49.81	47.12
Nb	8.83	0.30	0.25	0.77	0.11	0.71	0.58	0.88	19.44	1.80	3.98	2.73
Cs	0.24	1.87	0.04	0.11	0.04	0.55	0.05	0.05	0.03	0.06	0.05	0.01
Ba	20.11	35.69	2.70	8.09	1.36	126.59	34.44	47.15	0.33	45.45	46.95	49.70
Hf	12.37	0.19	0.03	0.63	0.03	0.19	0.21	0.10	3.27	0.73	1.61	1.44
Ta	1.48	0.10	0.15	0.19	0.19	1.45	0.47	0.45	0.97	0.73	0.71	1.54
Pb	4.13	0.93	1.08	1.44	1.58	4.38	10.47	7.18	0.46	2.07	2.49	1.03
Th	2.32	0.03	0.02	0.15	0.02	0.21	0.19	0.10	0.82	0.09	0.36	0.09
U	0.76	0.03	0.71	0.28	0.39	0.05	0.78	54.23	0.20	0.05	0.12	0.03
La	29.42	0.18	0.15	1.39	0.05	10.11	2.86	2.06	3.94	2.02	6.50	3.48
Ce	61.25	0.48	0.35	3.28	0.15	15.56	4.53	2.84	13.20	5.66	17.18	9.55
Pr	7.40	0.09	0.05	0.52	0.02	1.44	0.50	0.28	2.59	1.00	2.85	1.63
Nd	27.53	0.46	0.21	2.49	0.09	4.27	1.85	1.10	14.27	4.95	12.63	7.93
Sm	5.88	0.16	0.07	0.83	0.04	0.53	0.37	0.18	5.31	1.48	3.32	2.39
Eu	1.65	0.03	0.02	0.22	0.01	0.48	0.28	0.24	0.26	0.92	1.05	0.92
Gd	6.12	0.26	0.12	1.06	0.07	0.66	0.49	0.28	6.95	1.71	3.78	2.96
Tb	0.86	0.05	0.02	0.19	0.01	0.05	0.07	0.04	1.16	0.30	0.60	0.53
Dy	4.75	0.34	0.13	1.24	0.09	0.21	0.47	0.24	6.55	1.80	3.63	3.32
Ho	0.93	0.09	0.03	0.30	0.02	0.04	0.11	0.06	1.39	0.42	0.80	0.79
Er	2.33	0.27	0.08	0.82	0.06	0.09	0.29	0.17	3.41	1.14	2.08	2.16
Tm	0.34	0.05	0.01	0.14	0.01	0.01	0.05	0.03	0.51	0.17	0.32	0.36
Yb	2.02	0.29	0.10	0.96	0.07	0.08	0.29	0.18	3.13	1.12	1.93	2.23
Lu	0.30	0.05	0.01	0.16	0.01	0.01	0.05	0.03	0.54	0.17	0.28	0.36
(La/Yb)N	9.81	0.41	1.03	0.98	0.47	89.24	6.65	7.91	0.85	1.21	2.27	1.05
(La/Sm)N	3.15	0.68	1.24	1.05	0.87	11.95	4.80	7.18	0.47	0.86	1.23	0.92
(Gd/Yb)N	2.44	0.71	0.96	0.90	0.75	7.00	1.35	1.30	1.79	1.23	1.58	1.07
Ti/Ti*	0.32	0.78	0.34	0.75	0.74	0.14	0.35	0.57	0.82	1.42	0.65	0.90
Eu/Eu*	0.84	0.40	0.56	0.72	0.62	2.48	2.02	3.21	0.13	1.77	0.91	1.06
Nb/Nb*	0.43	1.78	1.96	0.69	1.37	0.20	0.32	0.80	4.39	1.76	1.06	1.95
Ti/Zr	9	72	66	84	121	32	51	111	97	217	113	129
Zr/Y	19.88	2.43	1.49	2.46	2.05	7.80	2.57	2.03	3.79	2.37	2.40	2.25
Al ₂ O ₃ /TiO ₂	23	18	13	25	16	571	389	345	4	27	16	17

Table 1 continued.

Sample	Amphibolite									
	df496634	df496635	df496642	df496645	df496650	df496656	hs0485223	hs0485224	hs0485225	hs0485234
SiO ₂	50.41	48.84	46.42	45.66	48.02	50.41	47.19	49.45	46.90	48.08
TiO ₂	1.45	0.50	0.82	0.44	0.58	0.74	0.74	0.71	0.90	0.76
Al ₂ O ₃	15.41	10.73	16.79	9.86	17.88	15.06	13.40	15.04	14.32	16.83
Fe ₂ O ₃	4.31	2.83	2.13	5.90	3.64	3.60	2.06	1.95	2.86	2.59
FeO	7.83	8.28	10.04	6.61	4.79	6.22	9.78	8.67	9.89	7.68
FeOt	11.71	10.82	11.95	11.92	8.06	9.46	11.63	10.43	12.46	10.01
MnO	0.19	0.20	0.19	0.17	0.15	0.18	0.22	0.18	0.20	0.16
MgO	5.93	16.75	6.72	23.62	7.09	7.56	9.68	8.21	7.43	7.15
CaO	9.08	7.68	12.55	5.42	14.03	12.09	12.78	11.82	13.55	12.21
Na ₂ O	3.14	1.73	1.51	0.69	1.87	2.14	1.45	1.76	1.90	1.83
K ₂ O	0.44	0.05	0.68	0.15	0.25	0.46	0.19	0.14	0.23	0.38
P ₂ O ₅	0.11	0.02	0.05	0.05	0.04	0.04	0.03	0.05	0.06	0.06
LOI	1.12	1.19	1.46	0.60	1.10	1.18	1.58	1.44	1.61	1.80
Sum	99.42	98.80	99.36	99.18	99.43	99.68	99.08	99.41	99.83	99.53
Mg#	47.40	73.40	50.10	77.90	61.10	58.70	59.70	58.40	51.50	56.00
Sc	41	46	38	13	39	46	46	39	43	37
Ti	9,124	2,627	4,424	2,172	3,187	3,925	4,155	4,189	5,326	4,792
V	299	189	252	96	186	277	275	211	236	221
Cr	149	1,350	249	1,833	757	466	413	265	217	492
Mn	1,547	1,660	1,605	1,433	1,215	1,531	1,778	1,464	1,610	1,339
Co	55	73	69	106	51	60	68	68	70	70
Ni	86	498	224	1,399	147	193	156	170	175	153
Cu	112	72	73	46	91	82	74	119	57	100
Zn	97	84	79	81	51	74	73	66	89	73
Ga	22.32	9.52	16.77	9.80	14.86	14.96	14.18	14.78	15.97	16.05
Rb	4.01	0.92	7.51	0.90	3.67	4.45	2.35	1.91	2.07	11.02
Sr	164.4	18.3	111.9	17.4	110.1	90.4	64.5	104.0	96.6	151.4
Y	29.15	11.66	19.08	8.58	12.87	17.82	17.01	17.70	21.51	18.42
Zr	95.33	23.35	44.87	39.49	31.90	35.02	31.37	39.59	43.14	44.28
Nb	4.00	1.07	2.19	1.98	1.36	1.82	1.40	1.63	2.12	2.14
Cs	0.05	0.01	0.04	0.04	0.21	0.14	0.09	0.04	0.18	0.66
Ba	45.39	7.03	74.57	11.11	23.66	63.94	19.55	21.57	31.00	33.28
Hf	2.71	0.75	1.28	1.01	0.83	1.05	0.91	1.18	1.34	1.32
Ta	0.90	0.48	0.69	0.33	0.36	0.45	0.27	0.35	0.29	0.37
Pb	3.29	0.39	2.21	0.71	1.08	4.13	0.66	1.64	0.84	3.42
Th	0.50	0.03	0.14	0.53	0.16	0.28	0.02	0.18	0.03	0.10
U	0.13	0.03	0.07	0.15	0.09	0.20	0.45	0.47	0.26	0.91
La	4.81	1.32	3.10	3.37	1.69	2.58	1.69	2.15	2.50	2.83
Ce	12.57	3.52	7.35	7.46	4.33	6.18	4.80	5.44	6.93	7.01
Pr	2.19	0.58	1.14	1.03	0.72	0.98	0.85	0.90	1.21	1.16
Nd	11.01	2.92	5.70	4.43	3.72	4.98	4.50	4.69	6.20	5.52
Sm	3.61	1.05	1.84	1.18	1.29	1.65	1.60	1.62	2.13	1.82
Eu	1.24	0.41	0.78	0.38	0.52	0.63	0.60	0.60	0.79	0.70
Gd	4.43	1.40	2.48	1.41	1.64	2.26	2.13	2.15	2.80	2.42
Tb	0.78	0.26	0.46	0.22	0.31	0.41	0.39	0.40	0.51	0.44
Dy	4.78	1.82	2.95	1.31	1.98	2.63	2.56	2.66	3.23	2.81
Ho	1.07	0.43	0.71	0.29	0.46	0.63	0.59	0.62	0.77	0.66
Er	2.81	1.20	1.86	0.79	1.26	1.69	1.59	1.74	2.01	1.79
Tm	0.43	0.20	0.29	0.13	0.20	0.27	0.26	0.28	0.33	0.30
Yb	2.66	1.28	1.91	0.79	1.26	1.75	1.61	1.79	1.95	1.84
Lu	0.41	0.19	0.29	0.12	0.20	0.28	0.25	0.28	0.30	0.30
(La/Yb)N	1.22	0.69	1.09	2.86	0.90	0.99	0.71	0.81	0.86	1.04
(La/Sm)N	0.84	0.79	1.06	1.80	0.82	0.98	0.67	0.83	0.74	0.98
(Gd/Yb)N	1.34	0.89	1.05	1.43	1.04	1.04	1.07	0.97	1.16	1.06
Ti/Ti*	0.90	0.83	0.80	0.68	0.86	0.78	0.87	0.87	0.84	0.89
Eu/Eu*	0.95	1.03	1.11	0.91	1.09	1.00	1.00	0.98	0.99	1.02
Nb/Nb*	1.05	2.22	1.35	0.60	1.07	0.87	3.05	1.06	3.13	1.60
Ti/Zr	96	112	99	55	100	112	132	106	123	108
Zr/Y	3.27	2.00	2.35	4.60	2.48	1.96	1.84	2.24	2.01	2.40
Al ₂ O ₃ /TiO ₂	11	21	20	22	31	20	18	21	16	22

Results - Geochemical characterization

Amphibolites

The mafic rocks of the Naujat gabbro-anorthosite complex are characterised by MgO (5.2–9.7 wt%), Mg-number (44–61), Ni (76–242 ppm), Cr (108–757 ppm). They have variations in SiO₂ between (46–50 wt.%), Al₂O₃ (14–23 wt.%), TiO₂ (0.6–1.0 wt.% with an outlier of 1.45 wt.%). The Al₂O₃/TiO₂ ratios are low (11–31) and the Zr/Y ratios show a wide range (1.84–3.27) but six of the eleven least altered amphibolitic samples cluster reasonably well around the chondritic Zr/Y ratio 2.4. The Ti/Zr ratios are (96–132 with an outlier of 217) and span around the chondritic value of 112.

The amphibolites are characterized by a relatively flat and uniform, weakly convex, rare-earth-element (REE) patterns of about 10 times the chondritic value on a chondrite-normalized diagram (Fig. 3a). There is also a slightly depleted to enriched rare-earth-element (LREE) pattern (La/Sm_N 0.7–1.0 excluding an outlier of 1.45) which is similar to modern N-MORB. Sample df 496605 is the only one showing a positive Eu anomaly.

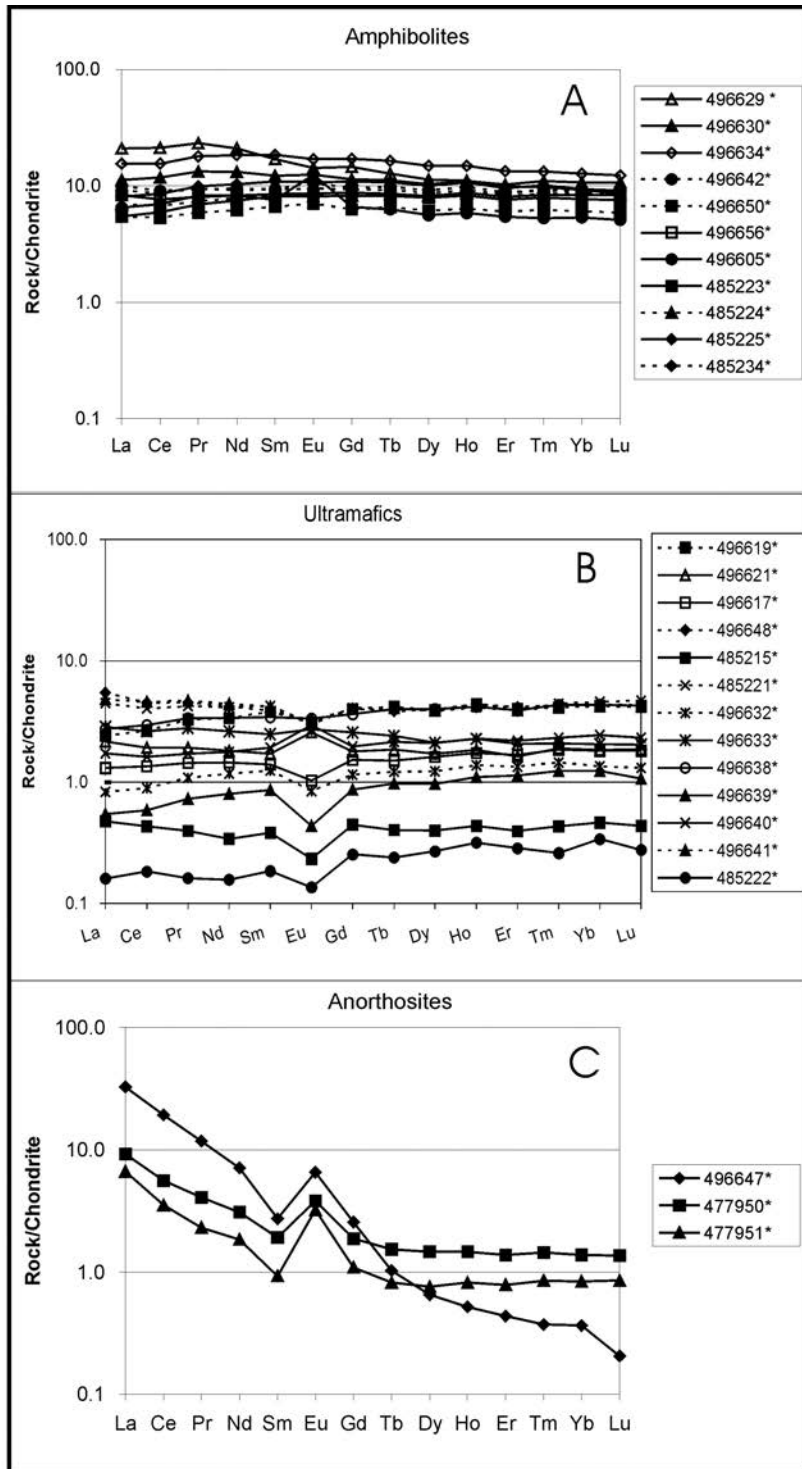


Figure 3. Chondrite normalized REE patterns of **a)** amphibolites, **b)** ultramafics and **c)** anorthosites. Chondrite normalising values from Boynton 1984.

On a primitive mantle-normalised trace element diagram (Fig. 4a) there is a pronounced variably negative Th anomaly and. The overall pattern shows a uniform and flat level besides minor negative Zr and Ti anomalies ($Ti/Ti^* = 0.65\text{--}0.90$, one outlier with 1.45 – sample df496605; Table 1). However sample df496605, df496629 and df496634 does not consistently follow the general pattern (showing a slightly enriched to depleted LREE pattern)

but these samples have gained some element mobility and should only be regarded as indicative. A negative Th anomaly is consistent with N-MORB chemistry (Wilson, 1989) but also for subduction zones.

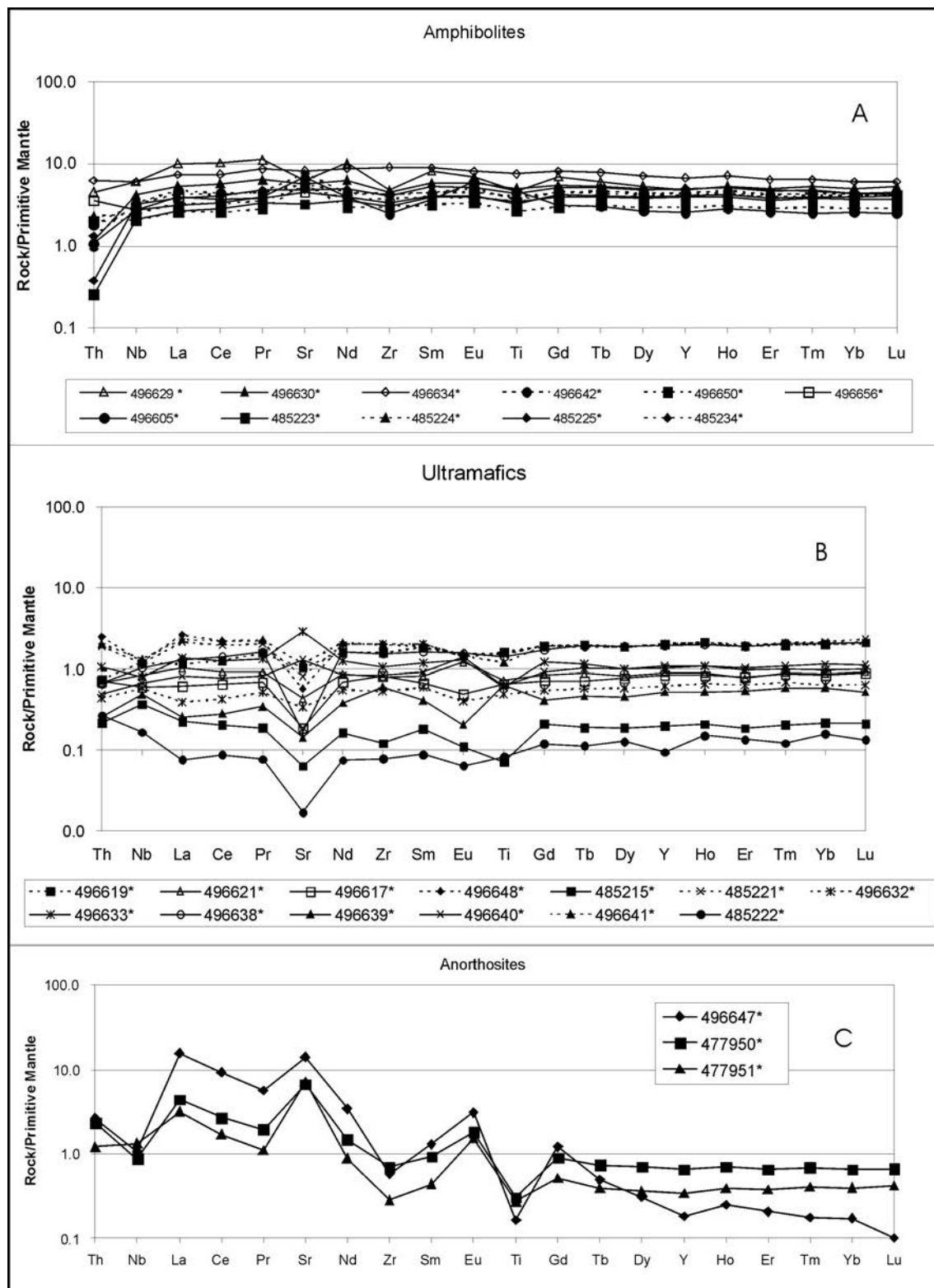


Figure 4. Primitive mantle normalized trace element diagrams of **a)** amphibolites, **b)** ultramafics and **c)** anorthosites. Normalisation values from McDonough and Sun (1995).

Several plots are made to classify the amphibolites and to discriminate their likely geological setting. All the amphibolites are classified as basalts according to the TAS-diagram (not shown) from LeMaitre et al. (1989). The AFM-diagram (Fig. 5.) after Irvine & Baragar (1971) show, that the basalts belong to the tholeiitic series, as it is also verified on a Jensen diagram, where they plot dominantly in the high-Mg tholeiitic basalt field (not shown; Jensen, 1976).

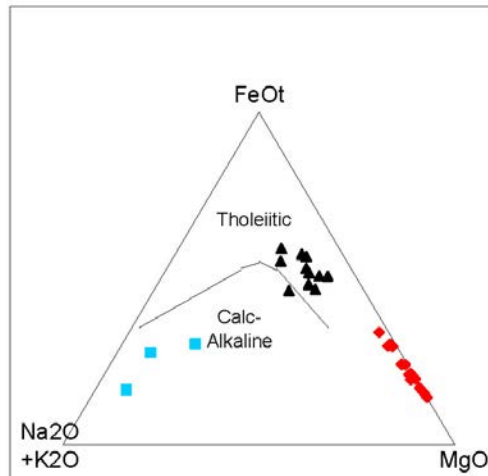


Figure 5. AFM-diagram of the least altered samples. Blue squares – anorthosites, black triangles – amphibolites, red diamonds – ultramafics.

Discrimination diagrams are used to differentiate between geological settings of the basalts. However, these discrimination diagrams are developed for modern-style tectonic settings and it is not certain if they account for the Archaean style geodynamic settings (van Krarkendonk 2003). A Ti-Zr-Y diagram (elements considered not to be mobile; Fig. 6) after Pearce & Cann (1973) shows, that our basalts do not plot as within-plate basalts but plot at the boundary between island-arc tholeiites and the field consisting of three types of settings (island-arc tholeiites – MORB – calc alkaline basalts). A Zr-Nb-Y diagram (Meschede 1986) further discriminates between basalts plotting all amphibolites in the field of N-MORB (Fig. 7).

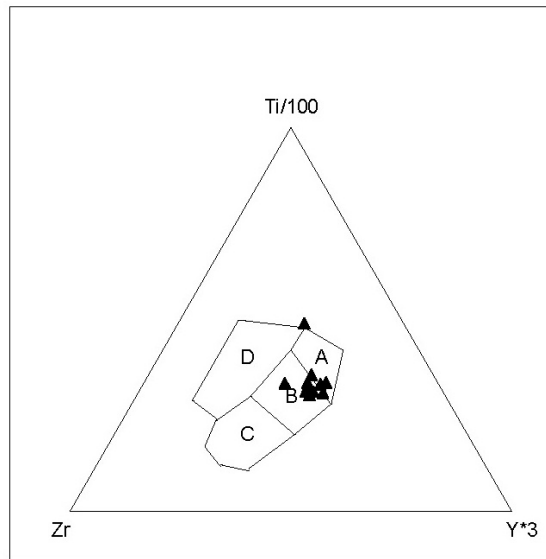


Figure 6. Amphibolites plotted in a Zr-Ti-Y diagram, after Pearce and Cann (1973). A - Island arc tholeiite, C – calc-alkali basalts, D – within-plate basalts and B – Island arc tholeiite, MORB and calc-alkali basalts.

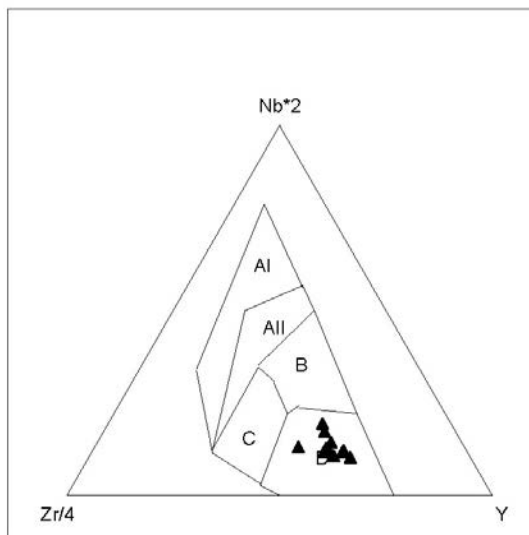


Figure 7. Zr-Nb-Y discrimination diagram for basalts, after Meschede (1986). AI – within-plate alkali basalts, AII within-plate alkali basalts and within-plate tholeiites, B – E-type MORB , C within-plate tholeiites and volcanic arc basalts, D - N- MORB.

Ultramafic rocks

The ultramafic rocks of the Naujat anorthosite complex are characterised by MgO (23–48 wt. %), Mg-number (77–91), Ni (887–3279 ppm), Cr (1534–3609 ppm) and SiO₂ (40–49 wt. %). The variations in Al₂O₃ are (0.6–9.4 wt. %) and in TiO₂ (0.04–0.4 wt. %.) yielding Al₂O₃/TiO₂ ratios 13–29. Ti/Zr ratios (65–122) span widely around the chondritic value of 112 and the Zr/Y ratios (1.89–2.48) are sub-chondritic to chondritic, with two outliers (ratios 1.49 and 2.82, sample hso485215 and df496639).

The ultramafic rocks have a high content of Cr and Ni and an increase in Ni with a positive linear trend versus MgO (Fig 8) possibly shows, that the Ni content is controlled by olivine content and fractionation (Wilson 1989) since olivine is a major host for Ni and the two samples with the highest Ni and MgO content are massive dunites.

The Chondrite-normalized REE patterns (Fig 3b) reflect olivine crystal fractionation (Wilson, 1989) positioning the general patterns from about 10 times the chondritic value depleted to about 10 times the chondritic value enriched (here the four most depleted samples are three dunites and one harzburgite). The patterns are, like the amphibolites, relatively flat and the HREE are slightly enriched compared to the LREE. All samples except 496621 and 496640 show a negative Eu anomaly.

The primitive mantle-normalised trace element diagram (Fig. 4b) display variable positive and negative anomalies for Nb, Sr, Eu and Ti. They have approximately the same characteristics as the amphibolites but show a more disturbed pattern which probably reflects larger element mobility.

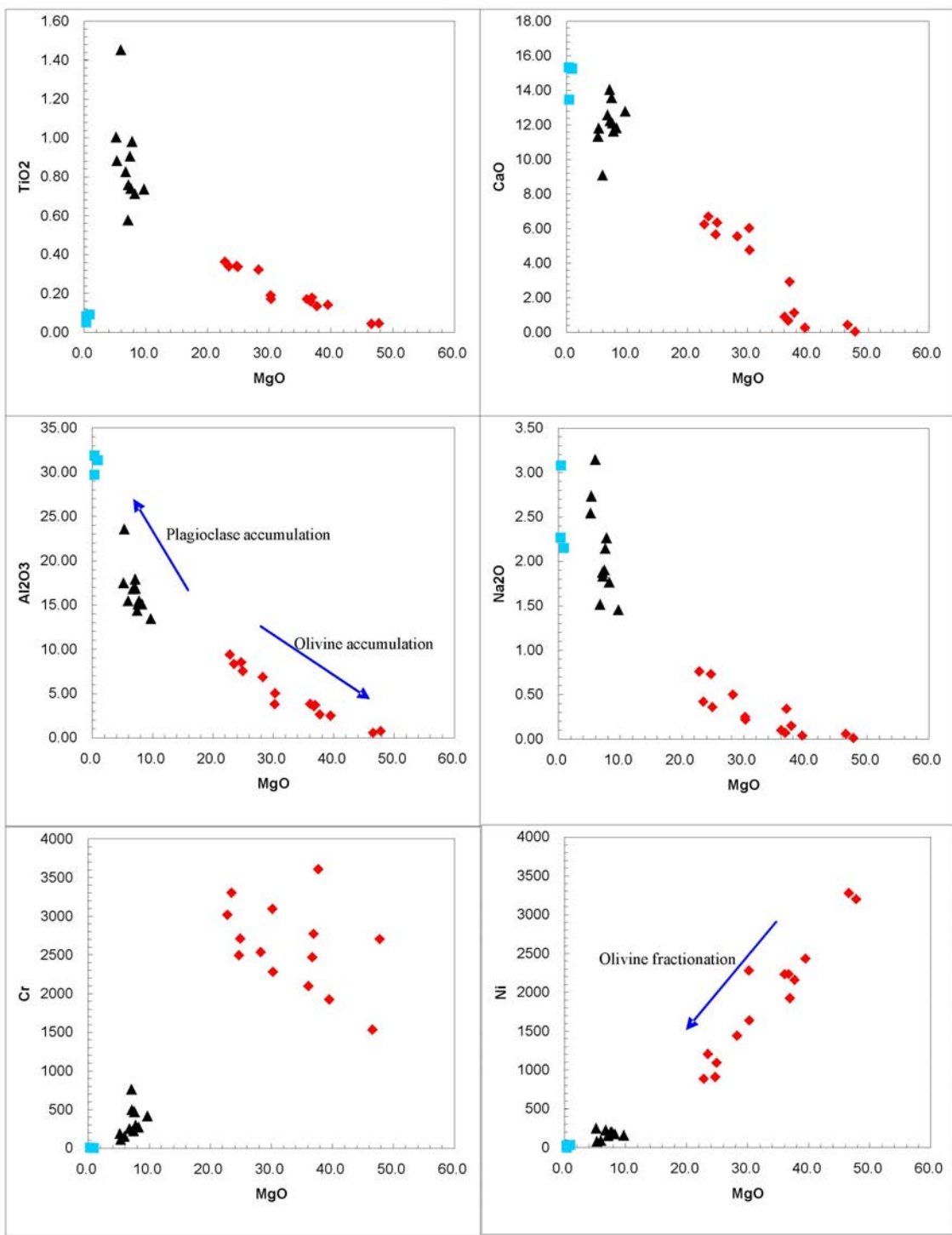


Figure 8. Variation diagrams of MgO vs. selected major- and trace elements. Symbols as in Fig. 5.

Anorthosites

The three analysed anorthosite samples are characterized by SiO_2 (48–52 wt.%), CaO (13.5–15.5 wt. %), Na_2O (2–5 wt.%) and Al_2O_3 are (30–32 wt.%). Sample df496647 is enriched in silica and depleted in CaO , Na_2O and Al_2O_3 with respect to the other two samples. In an MgO -variation diagram with MgO versus Na_2O (Fig. 8) there is a vertical spread where the silica-rich sample is enriched in Na_2O .

The chondrite-normalized rare-earth-element (REE) patterns of the anorthosite samples are enriched in the light-rare-earth-element (LREE) and show strong positive Eu anomalies (consistent with plagioclase in the mineralogy) and flat or slightly depleted heavy-rare-earth-element HREE contents (Fig. 3c). According to Ashwall & Myers (1994) these are typical characteristics of anorthosites. The trace element composition is consistent with other Archean anorthosite complexes (e.g. Nordlandet; Fiskenæsset, Bad Vermillion Lake; Ashwall & Myers 1994; Ashwall et al. 1983; Dymek & Owens 2001). The enriched LREE pattern (Fig. 3c) is similar to the granulite facies anorthosite in Nordlandet (Dymek & Owens 2001), which is suggested to have had olivine as an additional phase.

The most silica rich sample, df496647, show an increase of LREE and a depletion of HREE which also reflects the lower amount of mafic minerals (Dymek & Owens 2001).

Primitive mantle normalised trace element diagrams (Fig. 4c) shows the same pattern as for the REE with LREE enrichment and HREE depletion but also display positive La, Sr and Eu anomalies and negative Nb, Zr and Ti anomalies. Negative Ti anomalies might reflect Ti-oxide e.g. Ilmenite fractionation in the mantle source and Ilmenites are found in the ultramafic rocks. The positive Eu and Sr anomalies are typical for plagioclase rich rocks, because Eu^{2+} and Sr fit well into the mineral structure as substitutes of Ca.

Discussion

Alteration

All major units in the mapped area have been deformed during at least two major deformation events (Solgevik & Piazolo 2005) and have been metamorphosed under upper amphibolite to possibly granulite facies conditions. Thus, the sampled units have been deformed and metamorphosed to various degrees. Therefore, elements could have behaved mobile resulting in disturbance of the primary magmatic signatures. To assess possible alteration effects of the data that may result in misleading interpretations of e.g. geological environments, we have followed suggestions from Polat & Hofmann (2003) and plotted elements that are more mobile versus elements that mostly behave immobile (e.g Na₂O vs Zr). Outliers that are not included in a partition coefficient (R) of >0.75 have been screened out as altered and were not used for interpretation. Rb, Ba, U and Pb behave mobile during metamorphic processes. So they were excluded of the chondrite normalized trace element patterns and not used for further interpretation.

Following Polat & Hofmann (2003) sample df496658 was considered as altered because of the high LOI of more than 6 wt. %. Three samples of the ultramafic rocks (df496628, df496657, df496658) are ruled out due to petrographic evidence of alteration in combination with the above described criteria's. In total four ultramafic samples (df496604, df496628, df496657, df496658) are determined to be too altered for geochemical interpretations.

Samples 496603, 496635 and 496645 among the amphibolites are considered to be altered. They are mapped in the field as amphibolites and are mafic rich to heterogeneous amphibolites, they might resemble a cumulate transition phase between amphibolites-ultramafics as seen in the MgO-CaO-Al₂O₃ diagram (black triangles with high MgO content; Fig. 9) or they are altered varieties of amphibolites or ultramafics. The above listed amphibolites and ultramafics are therefore excluded from plots and diagrams interpretations from figure 3 and onwards in this report.

Beside the three altered amphibolites discussed above, samples df496605 df496629 and df496634, show some element mobility but follow roughly differentiation trends in the MgO variation diagrams (Fig. 8). They are not excluded from any diagrams but they are only considered as indicative in interpretations. Anorthosite sample 496647 is suggested to be altered due to e.g. silica enrichment and an increase in Na₂O compared to the other two anorthosite samples (Fig. 8).

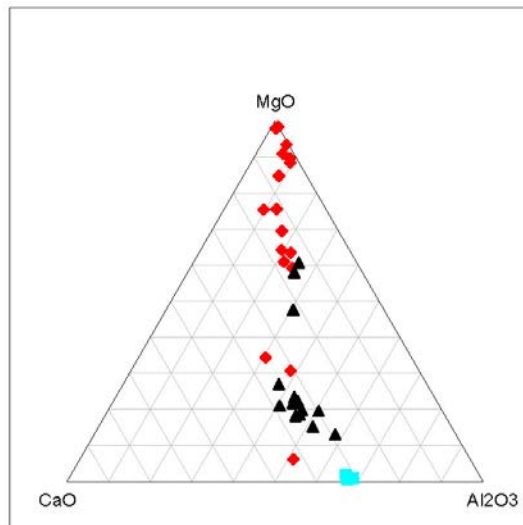


Figure 9. MgO - CaO - Al_2O_3 diagram of all samples.. Symbols as in Fig.5.

Major, trace and rare earth elements

The amphibolites are classified, according to discrimination diagrams as tholeiitic basalt with a possible origin of island-arc tholeiites or as oceanic crust (N-MORB) which may have the same source (Rollinson 1993).

The trace element and REE patterns of the amphibolites are comparable to those of tholeiitic basalts. Similar patterns were also found in the Ivisaartoq greenstone belt (Polat et al., 2007; Polat et al. in press;), on Nunataq 1390 (Stendal & Scherstén, 2007) and other greenstone associations in the Nuuk-region (Hoffmann, unpublished data; Hollis 2005). The Nb/Nb^{*}_{CN} (Table 1) are very variable. This could be an analytical artefact, because the largest scatter is recognized at Nb concentrations below 1 ppm. Therefore we do not use the Nb anomalies for the characterisation of the host magma in this report. A negative Nb anomaly would however be a signature for an island-arc environment and a negative Nb anomaly is found among the anorthosites, but not within the amphibolites or ultramafic rocks. Negative anomalies of Th and Zr are found in all three lithologies (except for the Zr in the ultramafic rocks). This could be interpreted as a subduction affinity of the magmas. However, negative Ti anomalies can be due to magnetite fractionation and are not a typical characteristic of subduction related sources.

The amphibolites show variability in the LREE, which varies from weakly depleted REE-patterns similar to modern N-MORB to enriched LREE patterns (La/Sm_N 0.7-1.45). This characteristic can be either the result of alteration processes or a primary characteristic of the mantle source. Due to the gabbroic texture in some of the amphibolite samples, these samples are most likely associated with the layered gabbro-anorthosite complex. This is also the case for the ultramafic rocks, because the sample suite shows clear olivine and plagioclase fractionation trends in MgO variation diagrams. The ultramafic rocks are most likely residual cumulates from the bottom of the magma chamber with the dunites as the most depleted rocks. On the basis of trace element patterns, it is not possible to distinguish the cumulative rocks from mantle rocks, which can have an overprint from subduction fluids. However, negative Zr and Th anomalies might also represent a subduction origin possibly related to island-arcs. To unravel this further high precision analysis of Nb and Ta are required.

Summary

Taking all chemical characteristics and field relationships into account, we suggest that the likely geological history of the Naujat anorthosite complex can be seen as:

- (1) Oceanic crust (now represented by amphibolite)
- (2) Intrusion of the gabbro-anorthosite complex in the upper oceanic crust with fractionation into cumulates, gabbros, leucogabbros and anorthosite.
- (3) Subduction of the complex or melting of the tholeilitic crust on the basis of thickened oceanic crust (?) with accompanied intrusion of TTG melts into the Naujat complex
- (4) Deformation
- (5) Intrusion of minor granitic melts
- (6) Deformation with large scale folding of the complex
- (7) Intrusion of pegmatites and doleritic dykes
- (8) Large scale faulting – probably Phanerozoic

In future projects, Lu-Hf and Sm-Nd isotope geochemistry shall be carried out on a suite of the least altered samples to date the anorthosite complex and the associated amphibolites directly. In addition, P/T-work and detailed studies of the mineral chemistry is planned. Also, geochronology of granitoids which intrude the Naujat complex will be carried out. Preliminary geochronology work on such granitoids has shown that the minimum age of the Naujat complex is around 2.78 Ga (Solgevik, unpublished data).

Acknowledgements

We would like to express our gratitude to Dirk Frei (GEUS) and Jens Konnerup-Madsen (University of Copenhagen) for their field work at the Naujat complex in 2006 and for providing us with the bulk of the samples for this study. The following persons were involved in field work during 2005-2007 (apart from the authors): Clark Friend, Susanne Schmidt and Sandra Piazolo (who also provided us with two samples). The Rock Geochemical Laboratory at GEUS is acknowledged for performing the XRF and ICP-MS analyses. Field work and analyses are financed by GEUS.

References

- Ashwall, L.D. & Myers, J. 1994: Archean Anorthosites. In: Condie, K.C. (ed.): Archean Crustal Evolution, Developments in Precambrian Geology **11**, Amsterdam-Lausanne-New York-Oxford-Schannon-Tokyo, Elsevier; 315–355.
- Ashwall, L.D., Morrison, D.A., Phinney, W.C. and Wood, J. 1983: Origin of Archean anorthosites: evidence from the Bad Vermilion Lake complex, Ontario. Contributions to Mineralogy and Petrology **82**, 259–173.
- Boynton, W.V. 1984: Geochemistry of the rare earth elements: meteorite studies. In: Henderson, P. (ed.): Rare earth element geochemistry, Amsterdam, Elsevier, 63–114.
- Dymek, R.F. & Owens, B.E. 2001: Chemical assembly of Archean anorthosites from amphibolite- and granulite facies terranes, SW Greenland. Contributions to Mineralogy and Petrology **141**, 513–528.
- Escher, J.C. & Pulvertaft, T.C.R. 1995: Geological map of Greenland, 1:2 500 000. Copenhagen: Grønlands Geologiske undersøgelse.
- Frei, D. & Konnerup-Madsen, J. 2007: Magmatic environment: The Naujat gabbro-anorthosite complex and country rocks – Field report 2006. In Stendal, H. (ed.): Characterization of selected geological environments. Mineral resource assessment of the Archaean Craton SW Greenland. Contribution no.1. Danmarks og Grønlands Geologiske Undersøgelse Rapport **2007/20**, 41– 58.
- Friend, C.R.L. & Nutman, A.P. 2005: New pieces to the Archean terrane jigsaw puzzle in the Nuuk region, southern west Greenland: Steps in transforming a simple insight into a complex regional tectonothermal model. Journal of the Geological Society, London **162**, 147–162.
- Hollis, J. (ed) 2005: Greenstone belts in the central Godthåbsfjord region, southern West Greenland. Geochemistry, geochronology and petrography arising from 2004 field work, and digital map data. Danmarks og Grønlands Geologiske undersøgelse Rapport **2005/42**. 215 pp.
- Irvine, T.N. & Baragar, W.R.A. 1971: A guide to the chemical classification of the common volcanic rocks. Canadian Journal of Earth Sciences **8**, 523–548.
- Jensen, L.S. 1976: A New Cation Plot for Classifying Subalkalic Volcanic Rocks. Ontario Division of Mines Miscellaneous Papers **66**, 22p.
- Kystol, J. & Larsen, L.M. 1999: Analytical procedures in the Rock Geochemical Laboratory of the Geological Survey of Denmark and Greenland. Geology of Greenland Survey Bulletin **184**, 59–62.
- LeMaitre, R.W. 1989: A classification of igneous rocks and glossary of terms. Blackwell Scientific Publication, Oxford. 193 pp.
- McDonough, W.F. & Sun, S.S., 1995: The composition of the Earth. Chemical Geology **120**, 223–253.
- Meschede, M. 1986: A method of discriminating between different types of mid-ocean ridge basalts and continental tholeiites with the Nb-Zr-Y diagram. Chemical Geology **56**, 207-218.
- Pearce, J.A. & Kann, J.R. 1973: Tectonic setting of basic volcanic rocks determined using trace element analysis. Earth and Planetary Science Letters **19**, 290–300.
- Polat, A. & Hofmann, A.W. 2003: Alteration and geochemical patterns in the 3.7–3.8 Ga Isua greenstone belt, West Greenland. Precambrian Research **126**, 197–218.

- Polat, A., Appel, P.W.U., Frei, R., Pan, Y., Dilek, Y., Ordóñez-Caldeeron, J.C., Fryer, B. and Raith, J.G., 2007: Field and geochemical characteristics of the Mesoarchean (~3075 Ma) Ivisaartoq greenstone belt, southern West Greenland: Evidence for sea-floor hydrothermal alteration in a supra-subduction oceanic crust. *Gondwana Research*, **11**, 69–91.
- Polat, A., Frei, R., Appel, P.W.U., Dilek, Y., Fryer, B., Ordóñez-Calderón, J.C. and Yang, Z. (in press): The origin and compositions of Mesoarchean oceanic crust: Evidence from the 3075 Ma Ivisaartoq greenstone belt, SW Greenland. *Lithos*, doi: 10.1016/j.lithos. 2007. 06.021.
- Rollinson, H., 1993. Using geochemical data: evaluation, presentation, interpretation. Longman Group UK Ltd. London, United Kingdom, 352 pp.
- Solgevik, H. & Piazolo, S. 2005: Field report from field season 2005, Kapsillit map-sheet. GEUS.
- Stendal, H. (ed.): Characterization of selected geological environments. Mineral resource assessment of the Archaean Craton SW Greenland. Contribution no.1. Danmarks og Grønlands Geologiske Undersøgelse Rapport **2007/20**, 88 pp.
- Stendal, H. & Scherstén, A., 2007: Geological environments: oceanic crust and hydrothermal alterations – Field report 2006. In Stendal, H. (ed.): Characterization of selected geological environments. Mineral resource assessment of the Archaean Craton SW Greenland. Contribution no.1. Danmarks og Grønlands Geologiske Undersøgelse Rapport **2007/20**, 59–88.
- Van Kranendonk, M.J., 2003: Archaean tectonics in 2001: an Earth odyssey. *Precambrian Research* **127**, 1–3.
- Weaver, B.L., Tarney, J., Windley, B.F. and Leake, B.E. 1982: Geochemistry and petrogenesis of Archaean metavolcanic amphibolites from Fiskenaesset, S. W. Greenland. *Geochimica et Cosmochimica Acta*. **46**, 2203–2215
- Wilson, M. 1989: Igneous petrogenesis. Chapman and Hall, London, 466 pp.